US Department of Energy and Lawrence Livermore Laboratory under Contract No. 2143103. The X-ray diffractometer was purchased with funds provided by the US National Science Foundation and by donors of the Foursight! program administered by the Oregon State University Foundation.

Reviews

New Luminescent Materials

G. Blasse

Debye Research Institute, University of Utrecht, PO Box 80.000,
3508 TA Utrecht, The Netherlands

Received March 8, 1989

Recent developments in the field of luminescent materials are reviewed. The role of luminescent rare-earth-metal ions has become predominant. Nevertheless certain classic topics, like Cr^{3+} luminescence and CdS luminescence, reappear, although in a different form. Attention is paid to luminescent materials for lighting, X-ray (storage) phosphors, scintillator crystals, Cr^{3+}-containing crystals and glasses, cryptates for medical diagnostics, and small semiconductor particles.

Introduction

Luminescent materials have a long history, in which chemistry plays an important role. Frequently new materials turn up that sometimes lead to important breakthroughs. Of current interest are the following groups of luminescent materials: phosphors for luminescent lighting,[1] where the classic halophosphate is replaced by mixtures of rare-earth-metal activated phosphors; X-ray phosphors for X-ray intensifying screens;[2] X-ray storage phosphors for digital radiography;[3] broad-band emitting crystals for use in tunable lasers; luminescent glasses and glass ceramics for lasers, fiber optics, solar concentrators, and lighting;[4,5] electroluminescent thin films;[6] cathode-ray phosphors that can withstand high excitation density (projection television);[7] scintillator materials;[7] the use of luminescent lanthanide ions as a probe for the structure of biological macromolecules.[8]

Research of luminescent materials has several aspects. There is, for example, the influence of sample preparation on the luminescence properties. Some materials are required in the form of large crystals of high quality, others in the form of powders with specific requirements on particle size distribution and morphology. Additionally, insight into the physics of the luminescence properties is required to obtain optimum properties in a controllable way. A special aspect is the way in which the luminescence properties depend on the chemical composition of the material.[7,9]

In this review we consider important developments in the field of luminescent materials during the past decade and wish to demonstrate that the study of luminescent materials is still challenging in spite of its long history. Some of these developments were possible because of a sufficient knowledge of the physics of the luminescent processes involved, while some appeared as surprises. In all cases the influence of chemical composition appeared to be of large importance.

Luminescent Materials for Lighting

Phosphors applied in luminescent lighting are excited by the short-wavelength ultraviolet radiation of a low-pressure mercury discharge (mainly 254 nm), which they convert into white light. Until 1975 the phosphor $Ca_5(PO_4)_3(F,Cl){:}Sb^{3+},Mn^{2+}$ (calcium halophosphate) was used. The UV radiation is absorbed by the Sb^{3+} ion and is reemitted as blue radiation. Those Sb^{3+} ions that are near to a Mn^{2+} ion transfer the excitation energy to Mn^{2+}, which emits yellow radiation. The color of the luminescence can be varied by varying the Mn^{2+} concentration. Roughly speaking, the more blue-emitting lamps give a higher light output, but the more yellow-emitting ones a better color rendering.[10]

In passing we note a recent study on the Sb^{3+} ion in halophosphate that shows that its luminescence is governed by the Jahn–Teller effect.[11]

In the early 1970s it was shown that the combination of three phosphors with narrow emission lines centered around 450, 550, and 610 nm, results in luminescent lamps that combine a high light output with a good color rendering.[12] Such luminescent materials can be realized by

---

(1) Smets, B. M. *J. Mater. Chem. Phys.* **1987**, *16*, 283.
(2) Brixner, L. H. *Mater. Chem. Phys.* **1987**, *16*, 253.
(3) Takahashi, K.; Miyahara, J.; Shibahara, Y. *J. Electrochem. Soc.* **1985**, *132*, 1492.
(4) Boulon, G. *Mater. Chem. Phys.* **1987**, *16*, 301.
(5) Andrews, L. J.; Beall, G. H.; Lempicki, A. *J. Lumin.* **1986**, *36*, 65.
(6) Leskela, M.; Tammenmaa, M. *Mater. Chem. Phys.* **1987**, *16*, 349.
(7) Blasse, G. *Mater. Chem. Phys.* **1987**, *16*, 201.
(8) Horrocks Jr., W. de W.; Sudnick, D. R. *Acc. Chem. Res.* **1981**, *14*, 384.
(9) Blasse, G. *Prog. Solid State Chem.* **1988**, *18*, 79.
(10) See, e.g.: Butler, K. H. *Fluorescent Lamp Phosphors*; Pennsylvania State University Press: University Park, 1980.
(11) Oomen, E. W. J. L.; Smit, W. M. A.; Blasse, G. *Mater. Chem. Phys.* **1988**, *19*, 357.
(12) Koedam, M.; Opstelten, J. J. *Light Res. Technol.* **1971**, *3*, 205.

0897-4756/89/2801-0294$01.50/0

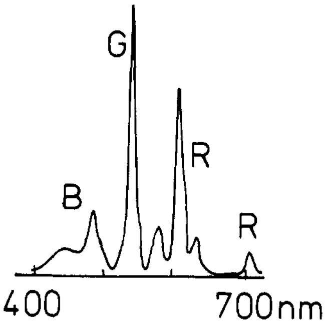

Figure 1. Emission spectrum of the blend of three phosphors in a three-color lamp. B, G, and R denote the dominant lines of the blue, green, and red emitting phosphors (after data in ref 13).

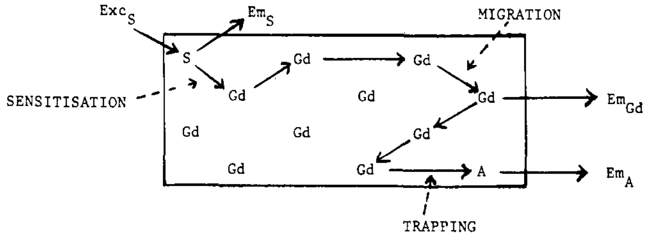

Figure 2. Schematic representation of the luminescence processes in a gadolinium compound: Exc, excitation; Em, emission; S, sensitizer; A, activator.

using rare-earth-metal ions as the luminescent ions.

The three-color lamp that was first realized uses the following phosphors (see also Figure 1): $BaMgAl_{10}O_{17}:Eu^{2+}$ with a narrow blue-band emission of Eu^{2+}; $CeMgAl_{11}O_{19}:Tb^{3+}$ with a line emission from Tb^{3+} in the green after UV excitation of Ce^{3+}; $Y_2O_3:Eu^{3+}$ with red line emission from Eu^{3+}.[13]

The first two phosphors are complex materials. This is illustrated by the fact that the composition of the blue-emitting phosphor was originally thought to be $BaMg_2Al_{16}O_{27}$.[13,14] Lamps made with these phosphors not only produce a high light output and a good color rendering but also have improved life. It is a fascinating observation that today lighting is taken care of by the rare-earth elements in many countries of the world.

The advent of the compact luminescent lamp led to the development of a new class of luminescent materials, such as those based on gadolinium compounds. There has been a lot of interest in energy migration in Gd^{3+} compounds, because this phenomenon opens interesting possibilities for new, efficient luminescent materials.[7,15] The Gd^{3+} sublattice is both sensitized and activated. The sensitizer(s) absorbs ultraviolet radiation efficiently and transfers it to the Gd^{3+} sublattice. By energy migration in this sublattice, the activator (A) is fed and emission results. Absorption and quantum efficiencies of over 90% have been attained. The physical processes can be presented schematically as follows (see Figure 2):

$$\xrightarrow{\text{exc}} S \rightarrow Gd^{3+} \xrightarrow{n\text{ times}} Gd^{3+} \rightarrow A \xrightarrow{\text{emission}}$$

A suitable choice of S is Ce^{3+}, Bi^{3+}, Pr^{3+}, or Pb^{2+}. For A, suitable choices are Sm^{3+}, Eu^{3+}, Tb^{3+}, Dy^{3+}, Mn^{2+}, or UO_6^{6-}, although there are probably many more.

We will discuss the energy-transfer phenomena in more detail by considering the systems $NaGdF_4:Ce,Tb$[16] and $LiGdF_4:Ce,Tb$.[17] Table I and Figure 3 show the transfer and radiative rates involved in these systems. Note the following: (i) in $LiGdF_4:Ce,Tb$ the overall $Ce^{3+} \rightarrow Gd^{3+}$ energy transfer is not efficient. This is due to the fact that there occurs back transfer from Gd^{3+} to Ce^{3+}. The emitting energy level of Ce^{3+} in $LiGdF_4$ lies low enough for this back transfer from Gd^{3+} to Ce^{3+}. This is due to the nature of the crystal-field splitting in the excited 5d configuration of the Ce^{3+} ion; not only is the cubic e level at a sufficiently low energy, but also the noncubic splitting (S_4 site symmetry) is large (see Figure 4). In $NaGdF_4:Ce,Tb$ the energy transfer is very efficient, as the emitting Ce^{3+} level is at higher energy, (ii) the Gd^{3+}–Gd^{3+} transfer rate (p_4) is much higher than the Gd^{3+} radiative rate (p_3). The number of Gd–Gd jumps during the lifetime of the excited state is p_4/p_3, i.e., about 50 000. Because the migration is a random-walk process, the diffusion length is about $(50\,000)^{0.5}d$ = 1000 Å, where d is the shortest Gd^{3+}–Gd^{3+} distance (~4 Å), (iii) the Gd^{3+}–Gd^{3+} transfer rate (p_4) is of the same order of magnitude as the Gd^{3+}–Tb^{3+} trapping rate (p_6).

Table I. Energy Transfer and Radiative Probabilities of the Systems $NaY_{0.98-x}Ce_{0.01}Tb_{0.01}F_4$ and $LiY_{0.98-x}Gd_xCe_{0.01}Tb_{0.01}F_4$ at Room Temperature[a]

probability	value in $NaGdF_4$, s^{-1}	value in $LiGdF_4$, s^{-1}
P_1	$(4 \pm 1) \times 10^7$	2.5×10^7
P_2	10^8	$(0.5–1.5) \times 10^8$
P_3	130	200
P_4	$10^{7\pm1}$	$> 10^{7\pm1}$
P_5	0	1.5×10^5
P_6	4×10^5	10^8
P_7	250	200

[a] Excitation is into the Ce^{3+} ion. The transfer rates are given for nearest-neighbor distances.[16]

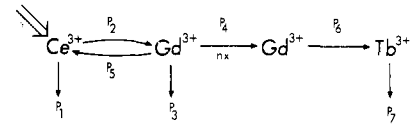

Figure 3. Radiative and transfer rates in a gadolinium compound (see also Table I).

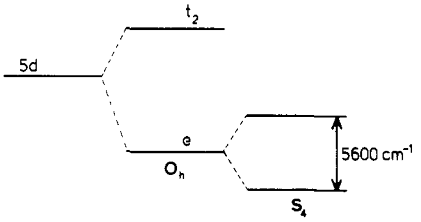

Figure 4. Crystal-field splitting of the 5d level of Ce^{3+} in $LiGdF_4$.

To function as a sensitizer, the Ce^{3+} ion should have its excited state at very high energy. To achieve this, the degree of covalency of the Ce^{3+}–ligand bond should be low and the crystal-field splitting of the excited 5d state should be small. For the coordination involved (~8), the latter requirement is usually fulfilled. The former requirement can be approached only approximately. Fluorides have been shown to be successful host lattices, as shown above (this holds also for $GdF_3:Ce$).[18] Borates are a second possibility, although, in many borates the Ce^{3+} emission is situated far below the lowest Gd^{3+} absorption level. High ionicity can be obtained by polarizing the borate

---

(13) Verstegen, J. M. P. J.; Radielovic, D.; Vrenken, L. E. *J. Electrochem. Soc.* **1974**, *121*, 1627.

(14) Smets, B. M. J.; Verlijsdonk, J. G. *Mater. Res. Bull.* **1986**, *21*, 1305.

(15) Blasse, G. *J. Less-Common Met.* **1986**, *126*, 139.

(16) Kiliaan, H. S.; Kotte, J. F. A. K.; Blasse, G. *J. Electrochem. Soc.* **1987**, *134*, 2359.

(17) Kiliaan, H. S.; Meijerink, A.; Blasse, G. *J. Lumin.* **1986**, *35*, 155.

(18) Blasse, G. *Phys. Status Solidi A* **1982**, *73*, 205.

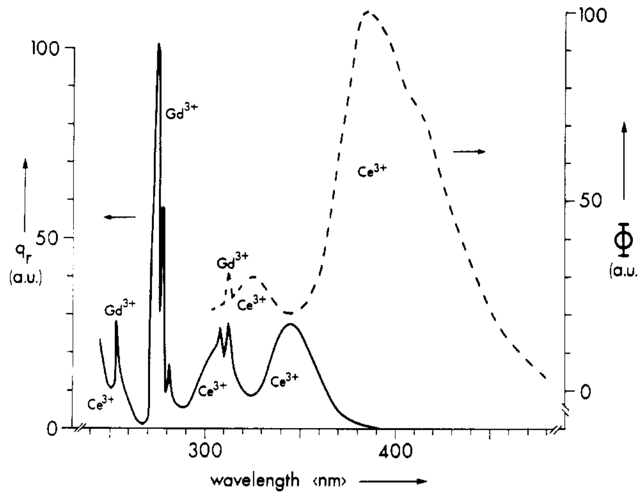

Figure 5. Luminescence spectra of $Li_6Gd(BO_3)_3$:Ce^{3+} at 300 K. Broken line: emission spectrum showing Ce^{3+} emission which is at too low energy to transfer to Gd^{3+}. Solid line: excitation spectrum of the Ce^{3+} emission, showing Ce^{3+} and Gd^{3+} transitions, the latter indicating $Gd^{3+} \rightarrow Ce^{3+}$ transfer. From: Kiliaan, H. S. Thesis, Utrecht, 1988.

groups that surround the Ce^{3+} ion in a direction away from the central Ce^{3+} ion, i.e., the borate groups should have highly charged ions with a small radius on the side opposite the Ce^{3+} ion. This simple model is remarkably successful.[19] In host lattices with condensed borate groups, the Ce^{3+} emission is at the required position ($GdMgB_5O_{10}$,[20] GdB_3O_6[21]). However, if this is not the case, the Ce^{3+} emission and absorption drops to such low values that it acts as an activator instead of a sensitizer (e.g., $Li_6Gd(BO_3)_3$:Ce,[19] see Figure 5). In less ionic compounds the Ce^{3+} levels are too low in energy, e.g., phosphates,[22] silicates,[23] and oxysulfate.[19]

The position of the Bi^{3+} and Pb^{2+} absorption bands is less easy to predict, but high ionicity seems to be required. The Bi^{3+} ion is a good sensitizer in GdB_3O_6[21] and Gd_2SO_6.[19] The Bi^{3+} ion has a large drawback, because it tends to form Bi^{3+} pairs and clusters that act as activators, since the energy levels of the pairs are at lower energy than those of the isolated Bi^{3+} ions.[19]

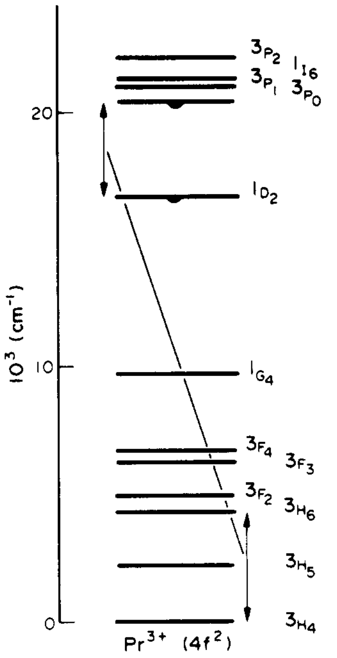

Figure 6. Energy level scheme of Pr^{3+}. Cross relaxation is indicated by arrowed lines.

Table II. Energy Migration Characteristics in Some Gd^{3+} Compounds at 300 K (after Ref 9)

compound	shortest Gd–Gd dist, Å	energy migration[a]	R_c, Å
GdF_3	3.7	+	$4.4 < R_c < 5.5$
$LiGdF_4$	3.8	+	$3.8 < R_c < 5.2$
$NaGdF_4$	3.6–3.9	+	$4.4 < R_c < 5.6$
$Gd_2O_2SO_4$	3.7	+	6.0
$Gd_3Li_3Te_2O_{12}$	3.8	+	$3.8 < R_c < 5.8$
Gd_2O_3	3.8	+	$5.4 < R_c < 6.6$
$GdMgB_5O_{10}$	4.0	+	~6.5
GdP_3O_9(O)	4.2	+	$R_c > 4.2$
$GdAl_3B_4O_{12}$	5.9	–	$5.9 < R_c < 7.3$
$LiGdP_4O_{12}$	5.6	–	
GdP_3O_9(M)	5.7	–	
$KGdP_4O_{12}$	6.6	–	
$Cs_2NaGdCl_6$	7.6	–	
$[Gd \subset 2.2.1]^{3+}$	10	–	

[a] (+) energy migration takes place; (–) energy migration does not take place or is of no importance.

The Pr^{3+} ion is a special case. de Hair[24] was the first to show its sensitizing action on Gd^{3+}, and Banks et al.[25] showed this also to be the case in $GdBO_3$. The conditions for efficient Pr^{3+}–Gd^{3+} transfer are rather critical.[26] To understand this, we have to consider the energy level scheme of Pr^{3+} ($4f^2$) (see Figure 6). The energy levels originating from the $4f^2$ configuration extend to 22 500 cm^{-1}. There is one left ($^1S_0$), but it is situated at much higher energy, viz., 47 000 cm^{-1}. However, the 4f5d configuration will appear at energies below this, especially in oxides. The $4f^2 \rightarrow$ 4f5d transition has a high oscillator strength, since it is an allowed transition. It can be used to efficiently excite the 4f5d state. Transfer from this state to Gd^{3+} has to compete not only with radiative emission from Pr^{3+} but also with nonradiative return from the 4f5d state to the $4f^2$ configuration levels. Efficient transfer occurs only if the relaxation in the excited 4f5d state is restricted, i.e., if the Stokes shift of the emission is small and if this emission overlaps favorably with the $^8S \rightarrow {}^6I$ absorption transitions of the Gd^{3+} ion. This is the case in $BaY_4Si_5O_{17}$:Pr,[24] $GdBO_3$:Pr,[25] and $Li_6Gd(BO_3)_3$:Pr.[19] In $(Y,Gd)_3Al_5O_{12}$:Pr the $Pr^{3+} \rightarrow Gd^{3+}$ transfer efficiency is low due to an unfavorable spectral overlap. Back transfer was also reported to occur.[25] In $Gd_{9.33}(SiO_4)_6O_2$:Pr the $Pr^{3+} \rightarrow Gd^{3+}$ transfer efficiency is also low, but this time because the 4f5d $\rightarrow 4f^2$ relaxation rate is faster than the transfer rate.[26] It has been shown that even if the transfer rate is very high, as in $GdBO_3$:Pr, the sensitization with Pr^{3+} has certain drawbacks, because activators such as Eu^{3+} and Tb^{3+} show back transfer to the $4f^2$ levels of the Pr^{3+} ion.[27]

The critical distance for energy transfer between Gd^{3+} ions (R_c) appears to be 5–6 Å.[28] This means that at this distance the probability for transfer equals the probability

---

[19] Kiliaan, H. S.; Blasse, G. *Mater. Chem. Phys.* **1987**, *18*, 155.

[20] Leskelä, M.; Saakes, M.; Blasse, G. *Mater. Res. Bull.* **1984**, *19*, 151.

[21] Hao Zhiran, Blasse, G. *Mater. Chem. Phys.* **1985**, *12*, 257.

[22] Kiliaan, H. S.; Herwijnen, F. P. van; Blasse, G. *J. Solid State Chem.* **1988**, *74*, 39.

[23] Kiliaan, H. S.; Herwijnen, F. P. van; Blasse, G. *Mater. Chem. Phys.* **1987**, *18*, 351.

[24] Hair, J. Th. W. de *J. Solid State Chem.* **1980**, *33*, 33.

[25] Srivastava, A. M.; Sobieraj, M. T.; Ruan, S. K.; Banks, E. *Mater. Res. Bull.* **1986**, *21*, 1455.

[26] Vries, A. J. de; Blasse, G. *Mater. Res. Bull.* **1986**, *21*, 683.

[27] Vries, A. J. de; Blasse, G.; Pet, R. J. *Mater. Res. Bull.* **1987**, *22*, 1141.

[28] Vries, A. J. de; Kiliaan, H. S.; Blasse, G. *J. Solid State Chem.* **1986**, *65*, 190.

Table III. Rates of Energy Transfer (s^{-1}) in $LiGdF_4$:Tb at 300 K[32]

$Gd^{3+}(^6P_{7/2}) \rightarrow Gd^{3+}(^6P_{7/2})$	9×10^5
$Gd^{3+}(^6I_{7/2}) \rightarrow Gd^{3+}(^6I_{7/2})$	3×10^7
$Gd^{3+}(^6P_{7/2}) \rightarrow Tb^{3+}$	2×10^5
$Gd^{3+}(^6I_{7/2}) \rightarrow Tb^{3+}$	2×10^7

for radiative decay on the Gd^{3+} ion. Migration among Gd^{3+} ions in a Gd^{3+} compound can, therefore, occur only if the shortest Gd–Gd distance is less than R_c. Since this transfer is exchange mediated (see above), the transfer probability falls off rather rapidly for increasing distance. The energy migration characteristics of a variety of gadolinium compounds are summarized in Table II.

It is especially interesting that $LiGdP_4O_{12}$ (Gd–Gd = 5.6 Å) shows no migration,[29] whereas $GdAl_3B_4O_{12}$, with a longer Gd–Gd distance,[29] still shows some migration. Due to the absence of inversion symmetry on the Gd^{3+} ions in $GdAl_3B_4O_{12}$ (trigonal prismatic coordination), the highly forbidden $^6P \rightarrow {}^8S$ emission transition on Gd^{3+} in $GdAl_3B_4O_{12}$ contains more electric-dipole character than in $LiGdP_4O_{12}$, where the Gd^{3+} site symmetry more closely approaches inversion symmetry. This indicates a small dipolar contribution to the Gd^{3+}–Gd^{3+} transfer in case the site symmetry lacks inversion symmetry: the R_c value of 5 Å seems to hold for exchange interaction only, and that of about 6 Å holds if there is an electric-dipole contribution to the interaction. Once again this shows that energy migration in a system of identical trivalent rare-earth-metal ions occurs only over short distances.

After a discussion of the sensitization and the migration in Gd^{3+} compounds, the trapping of the migrating excitation energy by an activator should be discussed. It was studied for many possible ions in the host lattice $GdAlO_3$.[30] There are two groups of activators, viz., those that overlap the Gd^{3+} emission with an allowed transition and those that overlap the Gd^{3+} emission with a forbidden transition. The former group consists of Ce^{3+} (10^7 s^{-1}), Cr^{3+} (10^6 s^{-1}), Eu^{3+} (10^6 s^{-1}), and Tb^{3+} (10^5 s^{-1}), where the estimated trapping rate at 300 K is given between in parentheses. We are dealing with electric dipole–dipole interaction. The second group consists of Sm^{3+} and Dy^{3+} (10^4 s^{-1}), Tm^{3+} (from Gd^{3+} $^6I_{7/2}$, 10^3 s^{-1}), Tm^{3+} (from Gd^{3+} $^6P_{7/2}$, 0 s^{-1}), and Er^{3+} (10^2 s^{-1}). Here we are dealing with exchange interaction. Note that the trapping rate is much slower than the Gd^{3+}–Gd^{3+} transfer rate (10^7 s^{-1}). The vanishing Gd^{3+} ($^6P_{7/2}$) $\rightarrow$ Tm^{3+} transfer is due to the fact that the Tm^{3+} ion has no energy levels within 3000 cm^{-1} from the Gd^{3+} $^6P_{7/2}$ level.

This system is instructive due to the fact that the starting material Al_2O_3 contained 100 ppm Cr. It turns out that this small amount of Cr^{3+} is able to compete successfully for the migrating excitation energy with 1% dopant concentrations of the second group. The trapping rates follow the Förster–Dexter theory,[31] as is to be expected.

Recently the system $LiGdF_4$:Ce,Tb has been reinvestigated by de Vries et al.[32] using tunable ultraviolet laser excitation of the Gd^{3+} ion. Excitation was in the $^6P_{7/2}$ and in the $^6I_{7/2}$ levels of Gd^{3+}. It turned out that energy migration occurs over the lower $^6P_{7/2}$ but also over the higher $^6I_{7/2}$ levels. Table III gives the transfer rates observed. It is seen that the migration over the $^6I_{7/2}$ level is faster, which is probably due to a larger spectral overlap.

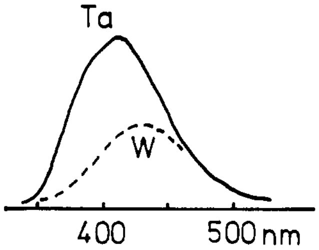

Figure 7. X-ray excited emission spectrum of $CaWO_4$(W) and $YTaO_4$:Nb(Ta). Curves are to scale.

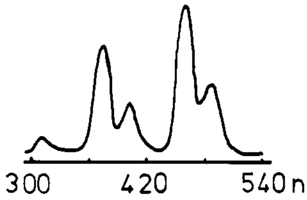

Figure 8. X-ray excited emission spectrum of LaOBr–Tm.

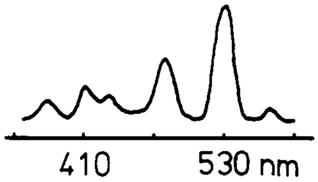

Figure 9. X-ray excited emission spectrum of Gd_2O_2S:Tb.

This type of research shows, once again, how in the field of luminescent materials the fundamental research is very close to the application. The present situation is such that there is sufficient knowledge to predict what the chemical composition of the most efficient gadolinium phosphors has to be. The final phosphor development has to select the composition that is the best for use in lamps.

Gadolinium compounds and rare-earth-metal ion luminescence play also an important role in the field of X-ray phosphors, which we would like to consider now.

X-ray Phosphors

Immediately after the discovery of X-rays by Röntgen in 1895, it was realized that this radiation is not efficient in exposing a photographic film. A search was started for phosphors that would absorb X-rays and, consequently, emit light efficiently in order to expose the film. The first X-ray phosphor was $CaWO_4$, which has been in use for over 70 years. Upon X-ray excitation it shows a blue broadband luminescence due to a charge-transfer transition in the tungstate group (Figure 7).

$CaWO_4$ has been replaced by rare-earth-metal activated phosphors. LaOBr:Tm^{3+} proved to be very effective in combination with blue-sensitive X-ray film.[33] Its emission consists of the sharp-line Tm^{3+} emissions in the ultraviolet and blue spectral regions (Figure 8). In combination with green-sensitive X-ray film, Gd_2O_2S:Tb^{3+} is a very good luminescent material.[34] Its emission is mainly in the green and blue spectral region and is due to the $^5D_4$–^7F_J transitions on the Tb^{3+} ion (Figure 9). Recently, the garnet $Gd_3Ga_5O_{12}$:Tb^{3+} has been proposed as an alternative.[35]

---

(29) Blasse, G.; Kiliaan, H. S.; Vries, A. J. de *J. Lumin.* **1988**, *40/41*, 639.

(30) Vries, A. J. de; Smets, W. J. J., Blasse, G. *Mater. Chem. Phys.* **1987**, *18*, 81.

(31) See, e.g.: *Energy Transfer Processes in Condensed Matter*; DiBartolo, B., Ed.; Plenum Press: New York, 1983.

(32) Vries, A. J. de; Hazenkamp, M. F., Blasse, G. *J. Lumin.* **1988**, *42*, 275.

(33) Rabatin, J. G. *Electrochem. Soc. Spring Meeting*, Toronto, Abstr, 1975, 198.

(34) Tekotzky, M. *Electrochem. Soc. Spring Meeting*, Boston, May 1968.

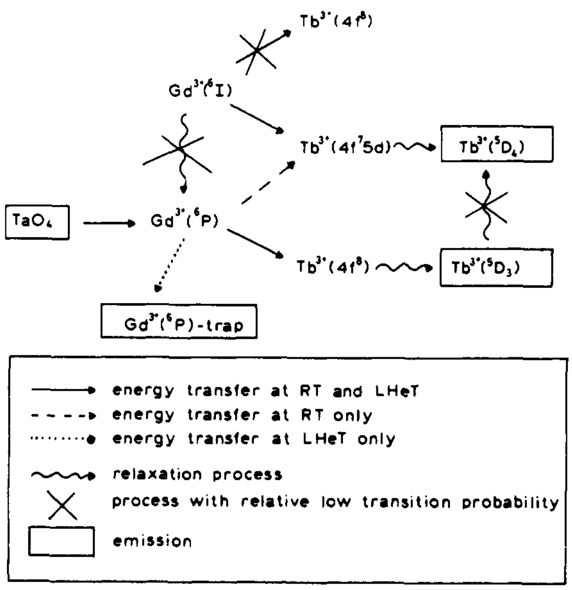

Figure 10. Luminescence processes in $GdTaO_4$:Tb. See also text. After: Lammers, M. J. J. Thesis, Utrecht, 1986.

A new family of X-ray phosphors is based on the M′ modification of $YTaO_4$,[2,36] which can be prepared with particle sizes useful for X-ray screens by using a Li_2SO_4 flux in the synthesis. M′-$YTaO_4$ shows an ultraviolet emission band with a maximum at 335 nm. This emission is due to a charge-transfer transition on the tantalate group. As an X-ray phosphor, M′-$YTaO_4$ is to be preferred over $CaWO_4$. Its density is higher (7.56 vs 6.06 $g\cdot cm^{-3}$) and its overall absorption characteristics are more favorable. This is mainly due to the Kα absorption edge of yttrium at 17.04 keV.[2] This advantage is augmented by replacing a small amount of tantalum with niobium. The emission shifts due to energy transfer from the tantalate to the niobate groups, which emit in the blue (Figure 7). This phosphor family is rather flexible. Instead of $YTaO_4$ one can also use $GdTaO_4$ (d = 8.81 $g\cdot cm^{-3}$) and $LuTaO_4$ (d = 9.75 $g\cdot cm^{-3}$). The latter is the densest, white, nonradioactive material. The composition $GdTaO_4$:Tb is a very efficient green-emitting photoluminescent and X-ray phosphor[2,36] (although not as good as Gd_2O_2S–Tb). From a fundamental point of view the large number of energy-transfer processes (see Figure 10) in $GdTaO_4$:Tb is interesting.[37] Excitation into the tantalate group is followed mainly by transfer to the Gd^{3+} ion (^6P levels). Energy migration over the ^6P levels ends up in Tb^{3+} ($4f^8$ configuration), resulting in blue ($^5D_3$) and green ($^5D_4$) Tb^{3+} emission. However, direct excitation into the higher ^6I levels of Gd^{3+} yields mainly green Tb^{3+} emission. This is due to the fact that migration occurs over the ^6I levels of Gd^{3+}, which transfer to the $4f^75d$ configuration of Tb^{3+}. From here the $^5D_4$ level of Tb^{3+} is reached directly. Finally, we note that $LuTaO_4$:Nb may find specific application in mammography, because even at low coating weights it is still very efficient when using the softer molybdenum radiation.[2]

A very recent development in this field is the use of Eu^{2+}-activated compounds as storage X-ray phosphors[3] (sometimes also called PSL (photostimulated luminescence) phosphors). These phosphors eliminate the need for a photographic film, because the excitation energy is stored inside them. Under photostimulation with a laser of suitable wavelength the stored energy is released as luminescence which is detected by a photomultiplier. The photomultiplier has a higher sensitivity than photographic film. Presently, the best example is BaFBr:Eu^{2+}.[3] Alternatives are $Ba_2B_5O_9Br$:Eu^{2+} [38] and especially $Ba_5SiO_4Br_6$:Eu^{2+}.[39]

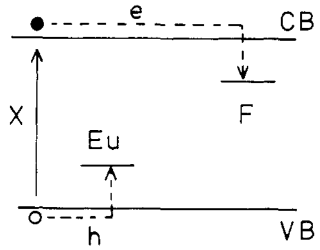

Figure 11. Simplified presentation of the storage action of BaFBr:Eu^{2+}. VB, valence band; CB, conduction band; X, free charge-carrier creation. The F center can be emptied by (red) laser excitation.

The physical mechanism is as follows (see Figure 11). Upon X-ray excitation free charge carriers are formed as well as F centers (Br vacancies). The holes are trapped by Eu^{2+}, converting them into Eu^{3+}. The electrons are trapped by the F centers. The stimulation occurs by optical excitation of the filled F centers, which promote their electrons to the conduction band. Upon recombination with the trapped holes, blue Eu^{2+} emission results. Recent studies indicate that the real mechanism is probably more complicated than the simple model presented here.[38,40]

Scintillator Crystals

Scintillator crystals are used to detect high-energy radiation such as γ-rays. The use of 12 000 crystals of $Bi_4Ge_3O_{12}$ at CERN (Geneva) has drawn attention again to scintillator crystals.[41] The Bi^{3+} ion shows a wide variability of luminescent properties.[7,8] We can distinguish three completely different situations:

(a) If the lattice relaxation of the excited state of the Bi^{3+} ion is very large, excitation and emission occur on the same Bi^{3+} ion, even if the bismuth concentration is high. This originates from the fact that the excited state after relaxation is far out of resonance with ions in the ground state. Since the excitation energy stays on the Bi^{3+} ion, this can be considered as an isolated ion. The spectra consist of broad bands, and the Stokes shift is very large. Examples are $LaPO_4$:Bi^{3+} and $Bi_4Ge_3O_{12}$.

(b) If the lattice relaxation is weaker than the interaction strength between the Bi^{3+} ions, i.e., if the Bi^{3+} wave functions show considerable wave function overlap, the luminescence properties have to be described by using a semiconductor model. Optical excitation results in the creation of free charge carriers (photoconductivity). These may recombine in different ways, e.g., free-exciton recombination, bound-exciton recombination, and deep-center recombination. A good example is $Cs_3Bi_2Br_9$ for which photoconductivity as well as narrow-line free-exciton emission has been observed.[42] Also, Bi_2O_3 and $Bi_{12}GeO_{20}$ are in this class.

---

(35) Lammers, M. J. J.; Severin, J. W., Blasse, G. *J. Electrochem. Soc.* **1987**, *134*, 2356.

(36) Brixner, L. H.; Chen, H. y. *J. Electrochem. Soc.* **1983**, *130*, 2435.

(37) Lammers, M. J. J., Blasse, G. *Mater. Res. Bull.* **1984**, *19*, 759.

(38) Meijerink, A.; Blasse, G. *Electrochem. Soc. Fall Meeting*; Chicago, Oct 1988, recent news paper 813; *J. Electrochem. Soc.* **1988**, *135*, 537C.

(39) Meijerink, A.; Blasse, G.; Struije, L. *Mater. Chem. Phys.* **1989**, *21*, 26.

(40) Seggern, H. von; Voigt, T.; Knüpfer, W.; Lange, G. *J. Appl. Phys.* **1988**, *64*, 1405.

(41) Rogemond, F.; Pédrini, C.; Moine, B.; Boulon, G. *J. Lumin.* **1985**, *33*, 455.

(42) Timmermans, C. W. M., Blasse, G. *Phys. Status Solidi B* **1981**, *106*, 647; *J. Lumin.* **1981**, *24/25*, 75.

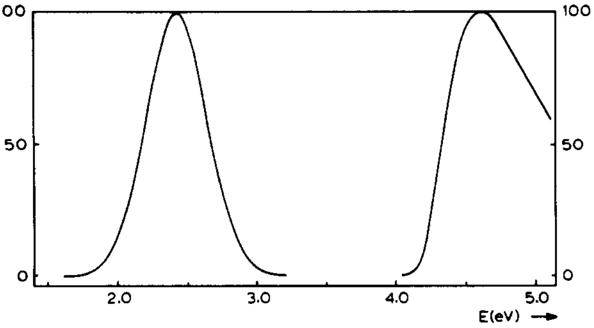

Figure 12. Emission and excitation spectra of the luminescence of $Bi_2Al_4O_9$. Note the large Stokes shift. After Timmermans, C. W. M. Thesis, Utrecht, 1983.

(c) If the relaxation as well as the interaction effect is weak, we have a situation that resembles that of the free ion more closely than the previous cases. Vibrational structure as well as energy transfer over large distances have been observed. Examples are Cs_2NaYCl_6–Bi^{3+} and $YAl_3B_4O_{12}$–Bi^{3+}.

Let us now return to $Bi_4Ge_3O_{12}$. We have argued that this compound belongs to the first class of materials,[43] although others have considered it to be of the semiconductor type. There now seems to be general agreement with our interpretation.[44] Actually there are many other compounds of this type, viz., $Bi_2Al_4O_9$, $Bi_2Ge_3O_9$, $PbAl_2O_4$, $PbGa_2O_4$,[8] $PbHPO_4$, $PbSO_4$,[45] and Pb decanoate.[46] Their Stokes shifts are surprisingly large, viz., about 2 eV. Figure 12 gives an example. The ion with s^2 configuration is coordinated asymmetrically in these compounds when it is in the ground configuration (pseudo-Jahn–Teller effect). Upon excitation, the chemical bond changes drastically, resulting in a more symmetrical coordination. This large reorganization is responsible for the large Stokes shift.[43]

In a physical sense, the situation is not different from that in the classical luminescent material $CaWO_4$. Actually the spectra look very much the same. This means that the configurational coordinate model must be used to interpret the luminescence. The Bi^{3+} center in $Bi_4Ge_3O_{12}$ belongs to the group of centers with strong coupling to the lattice. The Huang Rhys factor will be of the order of 20.

Whereas the scintillator $Bi_4Ge_3O_{12}$ can be described by the classic configurational coordinate model, there is a new class of scintillators that behave completely different. A characteristic example is BaF_2. It is used in positron emission tomography (PET), which is an in vivo tracer technique that uses the annihilation of positive electrons. By labeling compounds with positron emitters and introducing this into the body, it is possible to obtain a true three-dimensional image of the radioactivity distribution. High count rates and good time resolution are possible only if the scintillator emits with reasonable efficiency in the area $\lambda \leq 200$ nm with a very short decay time.[47]

Crystals of BaF_2 show two emissions with different characteristics, viz., an emission at 310 nm with a decay time of the order of a microsecond, which has been ascribed to self-trapped exciton decay, and an emission around 200 nm with a very fast decay (600 ps). The latter emission has been ascribed to "crossover transitions".[48,49]

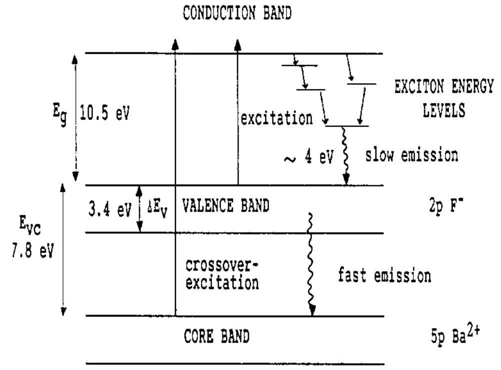

Figure 13. Schematic energy band scheme of BaF_2. See text. After Schotanus, P. Thesis, Delft, 1988.

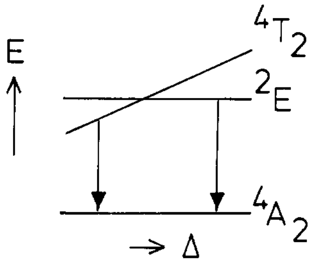

Figure 14. Energy levels of Cr^{3+} as a function of the crystal field Δ.

This theoretical explanation became feasible from synchrotron excitation experiments. The slow component appeared for excitation above about 10 eV, the fast one only for excitation above about 18 eV. The fast component corresponds to a recombination between a hole in the lower 5p (Ba^{2+}) band and an electron in the 2p (F^-) valence band (see Figure 13). The energy spacing between these two bands is less than between the valence and the conduction band, which is a neccessary condition for emission via crossover transitions. The structure in the emission has been described in terms of the density of states of the valence band. The intensity of the fast component is temperature independent between 100 and 800 K. These transitions are essentially localized and not greatly influenced by the presence of contaminations. Three components have been found at 220, 195, and 179 nm. Other compounds showing this effect are CsCl and CsBr.[50]

Another type of scintillator for this application is represented by the Nd^{3+}-doped fluorides. They show emission at about 175 nm due to an allowed d → f transition.[51] The decay time is a few nanoseconds.

There is rapid development of this area of luminescence involving completely different physics.

Luminescent Materials Activated with Cr^{3+}

The luminescence of ruby (Al_2O_3–Cr^{3+}) has inspired a large number of investigators for more than a century.[52] The first operational laser used a ruby crystal as the optically active medium. During the past decade there has

---

(43) Timmermans, C. W. M.; Blasse, G. *J. Solid State Chem.* **1984**, *52*, 222.

(44) Weber, M. J. *Proc. Int. Workshop on BGO*; Princeton University Press: Princeton, 1982; p 3; *Ionizing Radiat.* **1987**, *14*, 3.

(45) Blasse, G. *Phys. Status Solidi B* **1987**, *143*, K131.

(46) Burrows, H. D. *Mater. Lett.* **1988**, *6*, 191.

(47) Laval, M.; Moszynski, M.; Allemand, R.; Cormoreche, E.; Guinet, P.; Odru, R.; Vacher, J. *Nucl. Instrum. Methods* **1983**, *206*, 169.

(48) Aleksandrov, Yu. M.; Makhov, V. N.; Rodnyi, P. A.; Syreischikova, T. I.; Yakimenko, M. N. *Sov. Phys. Solid State* **1984**, *26*, 1734.

(49) Valbis, Ya. A.; Rachko, Z. A.; Yansons, Ya. L. *JETP Lett.* **1985**, *42*, 172.

(50) Valbis, Ya. A.; Rachko, Z. A.; Yansons, Ya. L. *Opt. Spectrosc.* **1986**, *60*, 679.

(51) Schotanus, P.; Eijck, C. W. E. van; Hollander, R. W.; Pijpelink, J. *Nucl. Instrum. Methods* **1985**, *A238*, 564. Schotanus, P.; Eijck, C. W. E. van; Hollander, R. W. *Nucl. Instrum. Methods A*, in press. Schotanus, P. Thesis, Technical University Delft, The Netherlands, 1988.

(52) See, e.g.: Imbusch, G. F.; Yen, W. M. In *Lasers, Spectroscopy and New Ideas, A tribute to A. L. Schawlow*; Springer-Verlag: Berlin, 1988; p 248.

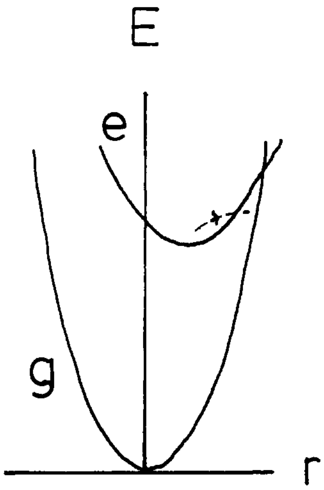

Figure 15. Configurational coordinate diagram for Cr^{3+} in a glass. The arrow indicates the nonradiative $^4T_2 \rightarrow {}^4A_2$ transition.

also been much interest in broad-band infrared emission of Cr^{3+} in crystals as well as glasses. Figure 14 shows the energy levels of the Cr^{3+} ion in an octahedral field as a function of the crystal-field strength. This diagram illustrates that high-field Cr^{3+} ions show $^2E \rightarrow {}^4A_2$ line emission (the situation in ruby), whereas low-field Cr^{3+} ions show $^4T_2 \rightarrow {}^4A_2$ band emission.

The broad-band emission of Cr^{3+} can be applied in laser materials to obtain tunable near-infrared emission[53] and in solar-energy concentrators.[54] In the latter system solar light is converted by Cr^{3+} into near-infrared emission. By using Cr^{3+} in a glass, this emission is trapped by total reflections and concentrated on a photovoltaic cell. The solar light is not only concentrated on the cell but also converted to the wavelength that is suitable for the photovoltaic cell. However, as we will see below, the Cr^{3+} quantum efficiency in a glass is not high enough to yield an acceptable concentration effect.

Research on Cr^{3+} broad-band emission comprises two interesting aspects, of which the first is the transition from line to band emission or from high-field to low-field Cr^{3+}. This aspect has been discussed in many papers. Let us mention here only some examples of materials that typically give line emission and of some that give band emission. Line emission is shown by $Al_2O_3{:}Cr^{3+}$, $MgAl_2O_4{:}Cr^{3+}$, β-$Ga_2O_3{:}Cr^{3+}$, and $LiAl_5O_8{:}Cr^{3+}$ and in general by Cr^{3+} ions substituted for small ions, so that a high-crystal field results due to short Cr–O distances. However, $YAl_3B_4O_{12}{:}Cr^{3+}$ is already on the borderline.[55] Broad-band emission has been found for $ScBO_3{:}Cr^{3+}$,[56,57] the garnets $Gd_3(Sc,Ga)_2Ga_3O_{12}{:}Cr^{3+}$, $(La,Lu)_3(Lu,Ga)_2Ga_3O_{12}{:}Cr^{3+}$,[58] and the elpasolites $Cs_2NaScCl_6{:}Cr^{3+}$ and $Cs_2NaYCl_6{:}Cr^{3+}$.[59] In these lattices the Cr^{3+} ion takes the place of a large host lattice ion, so that its crystal field is expected to be low.

The second aspect is the quantum efficiency of the Cr^{3+} broad-band emission, especially at room temperature. In crystalline lattices this efficiency can be high, even at 300 K. This is, for example, the case for $ScBO_3{:}Cr^{3+}$.[56] However, in glasses it is low, with a maximum value of 25% in certain glass compositions[60,61] but usually much lower. The reason for this is becoming more and more clear. Broad-band emission implies a considerable offset between the two parabolas in the configurational coordinate diagram (Figure 15). Especially if the excited state is at low energies which is the case for near-infrared emission, the rate for the nonradiative process becomes high.[62] In glasses the offset is expected to be larger than in crystals. The surroundings are less stiff and the luminescent ion less restricted in the choice of the site in case of a glass.[63,64]

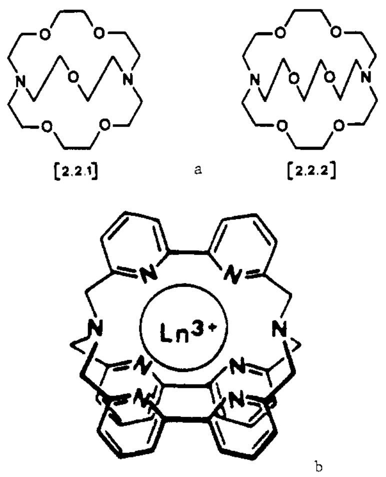

Figure 16. (a) The 2.2.1 and 2.2.2 cryptands. The central metal ion has been removed for clarity. (b) The $[Ln \subset bpy.bpy.bpy]^{3+}$ cryptate. The CH_2 groups are not indicated in these formulas.

This offset can be indirectly measured from the Stokes shift which is the energy difference between the maximum of the lowest excitation (absorption) band and the emission band. Imbusch[63] gives for the Stokes shift of Cr^{3+} broad-band emission for glasses typically 5000 cm^{-1} and for crystalline lattices typically 3000 cm^{-1}. That broad-band emission and excitation in glasses can be very inefficient processes from the point of view of the luminescence efficiency has been shown in our laboratory for several luminescent ions (Eu^{3+}, $UO_2{}^{2+}$, Cr^{3+}, Bi^{3+}).[65]

It has been shown that Cr^{3+}-containing glass ceramics show much higher quantum efficiencies.[66,67] A glass ceramic contains very small crystallites in the glassy phase. They remain transparent if these crystallites are small enough. The Cr^{3+} ion prefers to enter the crystalline phase, and in this way the efficiency can be increased considerably. The question remains whether the small amount of scattering that will occur is still acceptable for the intended application.

Cryptates in Medical Diagnostics

In recent years there has been considerable interest in the rare-earth-metal cryptates.[68] A cryptand is an organic cagelike molecule that can bind a rare-earth-metal ion in the cage (Figure 16). The cage presents some interesting properties of use for a luminescent material:

---

(53) See, e.g.; Jenssen, H. P.; Lai, S. T. *J. Opt. Soc. Am.* **1986**, *B3*, 115.

(54) Reisfeld, R.; Jørgensen, C. K.; *Struct. Bonding* **1982**, *49*, 1.

(55) Kellendonk, F.; Belt, T. van den; Blasse, G. *J. Chem. Phys.* **1982**, *76*, 1194.

(56) Lai, S. T.; Chai, B. H. T.; Long, M.; Morris, R. C. *IEEE J. Quantum Electron.* **1986**, *22*, 1931.

(57) Blasse, G.; Dirksen, G. J. *Inorg. Chim. Acta* **1988**, *145*, 303.

(58) Petermann, K., Huber, G. *J. Lumin.* **1984**, *31/32*, 71.

(59) Knochenmuss, R.; Reber, C.; Rajasekharan, M. V.; Güdel, H. U. *J. Chem. Phys.* **1986**, *85*, 4280.

(60) Andrews, L. J.; Lempicki, A.; McCollum, B. C. *J. Chem. Phys.* **1981**, *74*, 5526.

(61) Die, A. van; Leenaers, A. C. H. I.; Blasse, G.; Weg, W. F. van der *J. Non-Cryst. Solids* **1988**, *99*, 32.

(62) Blasse, G. In *Radiationless Processes*; Di-Bartolo, B., Ed. Plenum Press: New York, 1980; p 287.

(63) Imbusch, G. F.; Glynn, T. J.; Morgan, G. P. *J. Lumin.* in press.

(64) Die, A. van Thesis, University of Utrecht, The Netherlands, 1987.

(65) Verweij, J. H. M.; Blasse, G. *J. Non-Cryst. Solids* **1989**, *107*, 49; and to be published.

(66) Andrews, L. J.; Beall, G. H.; Lempicki, A. *J. Lumin.* **1986**, *36*, 65.

(67) Boulon, G. *Mater. Chem. Phys.* **1987**, *16*, 301.

(68) Sabbatini, N.; Perathoner, S.; Balzani, V.; Alpha, B.; Lehn, J. M. In *Supramolecular Photochemistry*; Balzani, V., Ed.; Reidel: Dordrecht, 1987; p 187.

(i) It restricts expansion upon excitation (compare Figure 15). In this way nonradiative transitions can be suppressed. If the rare-earth-metal ion fits the cage, the Stokes shift and, therefore, the nonradiative rate are small. This has been shown experimentally for the case of [Ce $\subset$ 2.2.1]$^{3+}$.[69]

(ii) The cage shields the luminescent ion from its further surroundings. This is of considerable importance in aqueous solutions. The rare-earth-metal ion emission is easily quenched if high-frequency vibrations reside in the direct neighborhood of the ion.[9,70] Water molecules present very high vibrational frequencies and quench the greater part of the rare-earth-metal ion emission. This nonradiative loss can be suppressed by caging the ion.[68]

(iii) By use of cryptands with very high absorption strength, which transfer this energy to the rare earth-metal ion, it is possible to obtain a high luminescence output from the molecular unity. This has been realized by using cryptands containing 2,2′-bipyridine (bipy, Figure 16, ref 68). Excitation occurs into the bipy group, which relaxes to the lowest triplet state. From here the energy is transferred to, e.g., the Eu^{3+} ion, which subsequently shows red emission.

For the application a Eu^{3+}-containing cryptate that shows a strong ultraviolet absorption is bonded to an antibody that couples specifically to certain biomolecules. If the labeled antibodies find the biomolecules one is looking for, they bind to these molecules, which after suitable treatment of the sample, show up by the luminescent Eu^{3+} label. The technique is very sensitive, can compete with radioactive labeling, and finds application at the moment.

Small Particles

Finally, we mention the luminescence of small particles, especially of semiconductors. There is no doubt that this is a fascinating development in the field of physical chemistry, although it is too early to identify applications for these particles.

The essential point is that the physical properties of small semiconductor particles are different from both the bulk and the molecular properties. It is generally observed that the optical absorption edge shifts to the blue if the semiconductor particle size decreases. This is ascribed to the quantum size effect. This is most easily understood from the electron-in-a-box model. Due to their spatial confinement the kinetic energy of the electrons increases. This results in a larger band gap.[71]

As an example we mention here colloids of ZnS. They can be prepared with variable particle size (down to 17-Å diameter, which corresponds to particles containing about 60 molecules of ZnS).[72] The onset of the optical absorption shifts from 334 nm (large particles and bulk) to 288 nm (17-Å particles). The particles show luminescence. Also the emission maximum shifts to shorter wavelength if the particle size is decreased.[72]

A recent, well-defined example of such clusters is the existence of CdS superclusters in zeolites.[73,74] The authors prepared very small CdS clusters in zeolites. In zeolite Y, for example, there are sodalite cages (5 Å) and supercages (13 Å). Well-defined clusters can be made by using these cages. The zeolites were Cd^{2+} ion exchanged and subsequently fired in H_2S. The resulting zeolite is white (note that CdS is yellow). The products were characterized by several means. It was shown that CdS is within the zeolite pore structure. There are discrete $(CdS)_4$ cubes in the sodalite cages. The cubes consist of interlocking tetrahedra of Cd and S. For high enough CdS concentrations these clusters are interconnected. As this interconnection proceeds, the absorption spectra shift in band edge from 290 to 360 nm. These materials show luminescence. Three different emissions have been observed, viz., a yellow-green (ascribed to Cd atoms), red (ascribed to sulfur vacancies), and blue (ascribed to shallow donors). A very interesting aspect is that the vibrational mode responsible for the nonradiative transitions in these materials has a frequency of 500–600 cm^{-1}. This is higher than the highest phonon frequency in CdS. This indicates that interface and host (zeolite) phonons are responsible for these processes.

No doubt these semiconductor superclusters present a novel class of materials where the three-dimensional structure can be controlled. They present a challenge to synthetic and physical chemists.

Conclusions

The developments in some classes of widely divergent luminescent materials have been reviewed. In many of these rare-earth-metal ions play the dominant role. In some others, however, we meet a classical activator (Cr^{3+}) or luminescent material (CdS) under completely new circumstances. This field has now reached a mature level where physical understanding in combination with synthetic abilities still yield new possibilities.

---

(69) Blasse, G.; Dirksen, G. J.; Sabbatini, N.; Perathoner, S. *Inorg. Chim. Acta* **1987**, *133*, 167.

(70) See, e.g., Blasse, G.; Sabbatini, N. *Mater. Chem. Phys.* **1987**, *16*, 237.

(71) See, e.g., Nozik, A. J.; Williams, F.; Nenadovic, M. T.; Rajh, T.; Micic, O. I. *J. Phys. Chem.* **1985**, *89*, 397.

(72) Weller, H.; Koch, U.; Gutierrez, M.; Henglein, A. *Ber. Bunsen-Ges. Phys. Chem.* **1984**, *88*, 649.

(73) Wang, Y.; Herron, N. *J. Phys. Chem.* **1988**, *92*, 4988.

(74) Herron, N.; Wang, Y.; Eddy, M. M.; Stucky, G. D.; Cox, D. E. Moller, K.; Beiz, T. *J. Am. Chem. Soc.* **1989**, *111*, 530.